Editors' Suggestion

Evidence for a New Structure in the $J/\psi p$ and $J/\psi\bar{p}$ Systems in $B_s^0 \to J/\psi p\bar{p}$ Decays

R. Aaij *et al.*[*]
(LHCb Collaboration)

(Received 11 August 2021; revised 29 November 2021; accepted 5 January 2022; published 7 February 2022)

An amplitude analysis of flavor-untagged $B_s^0 \to J/\psi p\bar{p}$ decays is performed using a sample of 797 ± 31 decays reconstructed with the LHCb detector. The data, collected in proton-proton collisions between 2011 and 2018, correspond to an integrated luminosity of 9 fb^{-1}. Evidence for a new structure in the $J/\psi p$ and $J/\psi\bar{p}$ systems with a mass of $4337^{+7\,+2}_{-4\,-2}$ MeV and a width of $29^{+26\,+14}_{-12\,-14}$ MeV is found, where the first uncertainty is statistical and the second systematic, with a significance in the range of 3.1 to 3.7σ, depending on the assigned J^P hypothesis.

DOI: 10.1103/PhysRevLett.128.062001

The observation of pentaquark candidates (P_c) in $J/\psi p$ final states produced in $\Lambda_b^0 \to J/\psi p K^-$ decays [1–3] by the LHCb experiment has stimulated interest in exotic spectroscopy. Recently, evidence for a structure in the $J/\psi\Lambda$ invariant-mass spectrum, consistent with a charmoniumlike pentaquark with strangeness, was found in $\Xi_b^- \to J/\psi\Lambda K^-$ decays [4]. The mass of these states is just below threshold for the joint production of a charm baryon and a charm meson, i.e., the $\Sigma_c\bar{D}^*$ and the $\Xi_c\bar{D}^*$ thresholds for the $J/\psi p$ and the $J/\psi\Lambda$ resonances, respectively. The mass separation from these thresholds might provide useful information for the phenomenological interpretation for these states. Proposed interpretation can be grouped into three classes: QCD-inspired models [5,6], residual hadron-hadron interaction models [7], and rescattering effects particle [8]. Additional measurements in different productions and decay channels are crucial to disentangle the various models [9].

The $B_s^0 \to J/\psi p\bar{p}$ decay was observed for the first time by the LHCb experiment in 2019 [10]. This channel may have sensitivity to the resonant P_c structures [1,2] within the $J/\psi p$ invariant-mass range of $[4034, 4429]$ MeV. Additionally, it could proceed via an intermediate glueball candidate $f_J(2220)$ decaying to $p\bar{p}$ [11]. Unlike $\Lambda_b^0 \to J/\psi p K^-$ decays receiving a relatively large contribution from the intermediate excited Λ resonances, no conventional states are expected to be produced in the B_s^0 decay, offering a clean environment to search for new resonant structures. Baryonic $B^0_{(s)}$ decays also allow for a study of the dynamics of the baryon-antibaryon system and its characteristic threshold enhancement, the origin of which is still to be understood [12].

In this Letter, an amplitude analysis of $B_s^0 \to J/\psi p\bar{p}$ decay is presented, including a search for pentaquark and glueball states, using proton-proton (pp) collision data at center-of-mass energies of 7, 8, and 13 TeV, corresponding to a luminosity of 9 fb^{-1}, collected between 2011 and 2018. The measurement is performed untagged, such that decays of B_s^0 and $\bar{B}_s^0$ are not distinguished and analyzed together.

The LHCb detector is a single-arm forward spectrometer covering the pseudorapidity range $2 < \eta < 5$, described in detail in Refs. [13–16]. The online event selection is performed by a trigger [17], comprising a hardware stage based on information from the muon system which selects $J/\psi \to \mu^+\mu^-$ decays, followed by a software stage that applies a full event reconstruction. The software trigger relies on identifying J/ψ decays into muon pairs consistent with originating from a B meson decay vertex detached from the primary pp collision point.

Samples of simulated events are used to study the properties of the signal and control channels. The pp collisions are generated using PYTHIA [18] with a specific LHCb configuration [19]. Decays of hadronic particles and interactions with the detector material are described by EvtGen [20], using PHOTOS [21], and by the GEANT4 toolkit [22,23], respectively. The signal $B_s^0 \to J/\psi p\bar{p}$ decays are generated from a uniform phase space distribution, while the $B_s^0 \to J/\psi\phi(\to K^+K^-)$ control mode is generated according to the model of Ref. [24].

The event selection follows the same strategy as Ref. [10]. Signal B_s^0 candidates are formed from two pairs of oppositely charged tracks. The first pair is required to be consistent with muons originating from a J/ψ meson with a decay vertex significantly displaced from its associated primary pp vertex (PV). For a given particle, the associated

[*]Full author list given at the end of the article.

PV is the one with the smallest impact parameter $\chi^2_{\rm IP}$, defined as the difference in the vertex fit χ^2 of a given PV reconstructed with and without the track under consideration. The second pair is required to be consistent with protons originating from the muon-pair vertex. A kinematic fit [25] to the B^0_s candidate is performed, with the dimuon mass constrained to the known J/ψ mass [26]. The selection is optimized using multivariate techniques [27] trained with simulation and data. Simulated events are weighted such that the distributions of momentum p, transverse momentum p_T, and number of tracks per event for B^0_s candidates match the $B^0_s \to J/\psi\phi$ control-mode distributions in data. In simulation the particle identification (PID) variables for each charged track are resampled as a function of its p, p_T, and the number of tracks in the event using $\Lambda_c^+ \to pK^-\pi^+$ and $D^{*+} \to D^0(\to K^-\pi^+)\pi^+$ calibration samples from data [28]. The selection consists of two boosted decision tree (BDT) classifiers. The first classifier, $\mathrm{BDT_{sel}}$, is a selection trained on $B^0_s \to J/\psi\phi$ simulation and sideband data with the $J/\psi p\bar{p}$ invariant mass above 5450 MeV using the p, p_T, and $\chi^2_{\rm IP}$ variables of the B^0_s candidate, the χ^2 probability from the kinematic fit of the candidate, and the impact parameter distances of the two muons. The second classifier, $\mathrm{BDT_{PID}}$, is trained on $B^0_s \to J/\psi p\bar{p}$ simulation and sideband data using proton identification variables: the hadron PID from the ring-imaging Cherenkov detectors, the p, p_T, and $\chi^2_{\rm IP}$ of the protons. The $\mathrm{BDT_{PID}}$ output selection criterion is chosen by maximizing the figure of merit $\mathcal{S}^2/(\mathcal{S}+\mathcal{B})^{3/2}$, where $\mathcal{S}$ and $\mathcal{B}$ are the signal and background yields in a region of ± 10 MeV around the B^0_s mass peak. These are determined from a fit to the $J/\psi p\bar{p}$ invariant-mass distribution in data after the $\mathrm{BDT_{sel}}$ selection, multiplied by the efficiency of the $\mathrm{BDT_{PID}}$ output requirement, obtained from simulation and from sideband data, respectively.

After applying these selection criteria, a maximum-likelihood fit is performed to the $J/\psi p\bar{p}$ invariant-mass distribution, shown in Fig. 1, yielding 797 ± 31 B^0_s signal decays. The B^0_s signal shape is modeled as the sum of two Crystal Ball [29] functions sharing a common peak position, with asymmetric tails describing radiative and misreconstruction effects. The signal-model parameters are determined from simulation and only the B^0_s peak position is allowed to vary in the fit to data. The combinatorial background is modeled by a first-order polynomial with parameters determined from the fit to data. The $B^0 \to J/\psi p\bar{p}$ component has the same shape as the B^0_s signal. The combinatorial-background fraction in the B^0_s signal window of 3σ around the mass peak ($[5357, 5378]$ MeV) is estimated to be $(14.9 \pm 0.6)\%$, where $\sigma \approx 3.5$ MeV is the resolution of the reconstructed invariant mass. The $m(J/\psi p)$ and $m(J/\psi \bar{p})$ invariant mass distributions of the reconstructed B^0_s candidates in the B^0_s signal region are shown in the bottom row of Fig. 2 (black dots), where hints

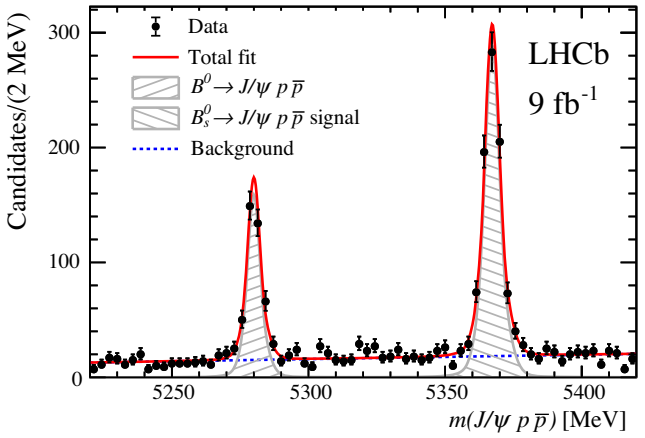

FIG. 1. Invariant-mass distribution $m(J/\psi p\bar{p})$ for reconstructed signal candidates; the result of the fit described in the text is overlaid.

of structure in the region around (4.3–4.4) GeV are present. This Letter investigates the nature of these enhancements, which are not compatible with the pure phase-space hypothesis.

An amplitude analysis of the B^0_s candidates is performed under the assumption of CP symmetry conservation; i.e., the dynamics is the same in B^0_s and $\bar{B}^0_s$ decays. Three

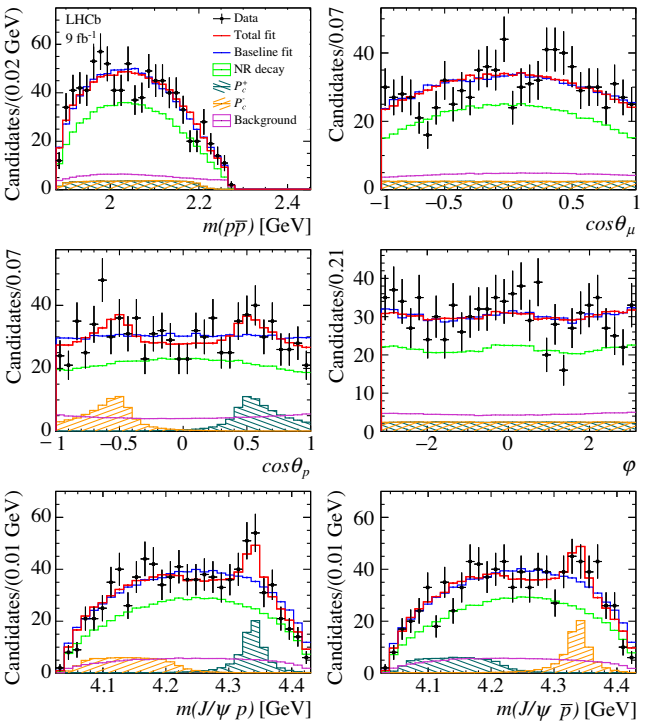

FIG. 2. One-dimensional projections of the angular $(\cos\theta_\mu, \cos\theta_p, \varphi)$ and invariant-mass distributions $[m(p\bar{p}), m(J/\psi p), m(J/\psi \bar{p})]$, superimposed with the results of the fit from the baseline model (blue) and the default model (red) comprising a NR term and the P_c contribution.

interfering decay sequences are considered in the amplitude model: $B_s^0 \to J/\psi X(\to p\bar{p})$, $B_s^0 \to P_c^+(\to J/\psi p)\bar{p}$, and $B_s^0 \to P_c^-(\to J/\psi \bar{p})p$, all followed by a $J/\psi \to \mu^+\mu^-$ decay. These sequences are labelled as the X, P_c^+, and P_c^- chains, respectively. Since the data sample is not flavor tagged, the distribution of the candidates in the phase space is by construction symmetric for $J/\psi p$ and $J/\psi \bar{p}$ final states, and therefore the analysis is sensitive to the sum of possible contributions from P_c^+ and P_c^- pentaquark candidates, denoted as P_c in the following. Because of the small sample size and since the B_s^0 or $\bar{B}_s^0$ flavor is not identified, there is no sensitivity to different couplings for the P_c^+ and P_c^- states, which are constrained to be equal, up to a phase difference. The amplitude model is based on the helicity formalism of Refs. [30,31], which defines a consistent framework for propagating spin correlations through relativistic decay chains. To align the spin of the different decay chains, the prescription in Ref. [32] is followed. Details about the amplitude definition are given in the Supplemental Material [33].

Candidates in the B_s^0 signal region are used to perform an amplitude fit in the four-dimensional phase space $(m_{p\bar{p}}, \vec{\Omega})$. This phase space is defined by the invariant mass $m_{p\bar{p}}$ of the $p\bar{p}$ pair and $\vec{\Omega} = (\theta_p, \theta_\mu, \varphi)$, where θ_p, θ_μ are the two helicity angles of the p and the μ^- in the X and J/ψ rest frame, respectively, and φ is the azimuthal angle between the decay planes, of the $\mu^-\mu^+$ and the $p\bar{p}$ pairs. The distributions of $(m_{p\bar{p}}, \cos\theta_\mu, \cos\theta_p, \varphi)$, together with the $m(J/\psi p)$ and $m(J/\psi \bar{p})$ invariant-mass projections, are shown in Fig. 2 for selected candidates.

The amplitude fit minimizes the negative log-likelihood function,

$$-2\log\mathcal{L}(\vec{\omega}) = -2\sum_i \log[(1-\beta)\mathcal{P}_{\rm sig}(m_{p\bar{p},i}, \Omega_i|\vec{\omega}) + \beta\mathcal{P}_{\rm bkg}(m_{p\bar{p},i}, \Omega_i)], \quad (1)$$

where the total probability density function (PDF) calculated for ith candidate has a signal $\mathcal{P}_{\rm sig}$ and a background $\mathcal{P}_{\rm bkg}$ component, where β is the fraction of background events observed within the B_s^0 signal window. The signal PDF is proportional to the matrix element squared, $|\mathcal{M}(m_{p\bar{p},i}, \Omega_i|\vec{\omega})|^2$, and depends on the fit parameters $\vec{\omega}$, i.e., the couplings, the masses, and the widths, which define the contributing resonances:

$$\mathcal{P}_{\rm sig}(m_{p\bar{p},i}, \Omega_i|\vec{\omega}) \equiv \frac{1}{I(\vec{\omega})}|\mathcal{M}(m_{p\bar{p},i}, \Omega_i|\vec{\omega})|^2\Phi(m_{p\bar{p},i})\epsilon(m_{p\bar{p},i}, \Omega_i). \quad (2)$$

The phase-space element is $\Phi(m_{p\bar{p},i}) = |\vec{p}||\vec{q}|$, where $\vec{p}$ is the momentum of the X system in the B_s^0 rest frame and $\vec{q}$ is the proton momentum in the X rest frame. The efficiency, $\epsilon(m_{p\bar{p},i}, \Omega_i)$, is included in the PDF, and is parametrized by a Legendre polynomial expansion on the four-dimensional phase space. The denominator, $I(\vec{\omega})$, normalizes the probability. The fit fractions of each signal component are defined as the corresponding PDF integral divided by $I(\vec{\omega})$. The background contribution $\mathcal{P}_{\rm bkg}$ is parametrized by the product of one-dimensional Legendre polynomials describing candidates in the B_s^0 sideband region of $[5420, 5700]$ MeV.

No well-established resonances are expected either in the $p\bar{p}$ or in the $J/\psi p$ and $J/\psi \bar{p}$ channels. However, some resonances could potentially decay into $p\bar{p}$ [26], e.g., the $f_J(2220)$ [34] and the $X(1835)$ [35,36]; thus they have been included in alternative models. The simplest model used to fit the data has no resonant contributions in the P_c^+, P_c^-, and X decay chains, and is denoted as the baseline model. This model includes a nonresonant (NR) contribution in the X decay sequence with spin-parity quantum numbers equal to $J^P = 1^-$, which has S-wave terms in both its production and decay. Indeed, due to the low Q value of the decay, the S-wave contribution is expected to be favored since higher values of orbital momentum are suppressed. Models including NR contributions with different quantum numbers (i.e., $J^P = 0^\pm, 1^+$) are excluded because their $-2\log\mathcal{L}$ values are significantly worse than that of the $J^P = 1^-$ hypothesis.

Because of the limited sample size, the baseline model is described by two independent LS couplings for both $B_s^0 \to J/\psi X$ and $X \to p\bar{p}$ decays, where L is the decay orbital angular momentum and S is the sum of spins of the decay products. Fixing the two lowest orbital momentum couplings as the normalization choice and three parameters, which are consistent with zero, reduces the number of free parameters to three.

The fit results of the baseline model are shown in Fig. 2. The baseline model does not describe the data distribution, with a χ^2 goodness-of-fit test result of $\chi^2/\text{d.o.f.} = 64/38$ corresponding to a p value of 4×10^{-5}. Therefore, two resonant contributions from P_c^+ and P_c^- are added, with identical masses, widths, and couplings. First, the $P_c(4312)$ state previously observed by the LHCb experiment in the $\Lambda_b^0 \to J/\psi p K^-$ analysis [2] is included in the model with mass and width fixed at their known values. The broad P_c structure with a mass around 4380 MeV, observed in 2015 [1], is not considered in this fit, since the helicity formalism used in Ref. [37] requires modifications in order to properly align the half-integer spin particles of different decay chains and, thus, those results need to be confirmed with an updated analysis of $\Lambda_b^0 \to J/\psi p K^-$ data [38,39]. In this analysis no evidence for the $P_c(4312)$ state is found since the p value, computed from the $-2\Delta\log\mathcal{L}$ of the alternative fit with respect to the default model, is measured to be 0.5. Exploiting the CL_s method [40], an upper limit on the modulus of its coupling is set to 0.043 at 90% of confidence level, which corresponds to a fit fraction of 2.86%. A model

with a new $P_c^{\pm}$ state given a free mass and width is chosen as the default model. Different spin-parity hypotheses for the P_c states are investigated, i.e., $J^P = 1/2^{\pm}$ and $J^P = 3/2^{\pm}$. Because of a limited sample size, only the lowest values of L are considered and the same coupling is assumed for all J^P hypotheses, resulting in two free parameters: the modulus $A(P_c)$ and the phase $\phi(P_c)$ of the coupling. The seven fit parameters $\vec{\omega}$ contain the baseline model parameters, see Eq. (2), the coupling $[A(P_c), \phi(P_c)]$, the mass, and width of the P_c state.

The fit result for the $J^P = 1/2^+$ hypothesis of the P_c^+ state is shown in Fig. 2. The χ^2/d.o.f. is 36.7/36.8, where the number of degrees of freedom (d.o.f.) is determined from fits to the χ^2 distribution extracted from pseudoexperiments. The statistical significance is estimated from pseudoexperiments generated with the baseline model and fitted with the default model, using amplitude parameters determined by the fit to data. The mass and width of the P_c states are not defined in the baseline model, thus multiple fits to the same pseudodata are performed to account for the look-elsewhere effect, scanning the initial mass value in intervals of size 50 MeV. The test statistic t is built as the maximum of the $-2\log\mathcal{L}$ difference between the baseline and the default model [41] among all the fits obtained by scanning the initial mass values. The p value is computed using a frequentist method as the fraction of pseudoexperiments with t larger than the t_{data} value from the fits to data. The p value ranges between 0.02% and 0.2% for different J^P hypotheses, the lowest being associated to $1/2^+$ and the highest to $3/2^+$, as reported in the Supplemental Material [33]. These p values correspond to a signal significance in the range of 3.1 to 3.7σ, providing evidence for a new pentaquarklike state. Using the CL_s method [40], none of the J^P hypotheses considered can be excluded at 95% confidence level.

The hypothesis of a glueball state with mass equal to 2230 MeV and width of around 20 MeV [11] is also tested, by adding to the default model a resonance in the X decay chain with fixed mass and width. No evidence of $f_J(2220)$ is observed, as the fit with this contribution gives a p value, computed from the $-2\Delta\log\mathcal{L}$ with respect to the default model, of 0.75 and an associated complex coupling of $[-0.04 \pm 0.09, -0.06 \pm 0.16]$.

Systematic uncertainties are evaluated for the mass, width, coupling, and fit fractions of the sum of the $P_c^{\pm}$ contributions. For each source of uncertainty, pseudoexperiments are generated according to the alternative model with the same sample size as in data. The fit to such pseudoexperiments is performed using the default model. The systematic uncertainties, listed in Table I, are assigned as the mean of the residual distributions between the fitted and the default parameter results. The main contributions are due to different NR models for the X decay chain, alternative J^P hypotheses for the P_c state, and possible mismodeling of the efficiency distribution. The systematic uncertainty associated to the NR model is obtained including, in addition to the NR term with $J^P = 1^-$ and lowest values of L allowed, a P-wave resonant contribution with $J^P = 0^-$, modeled with a Breit-Wigner line shape in order to account for possible resonances, such as the $X(1835)$ [35,36], decaying to a $p\bar{p}$ final state. Since none of the J^P hypotheses investigated for the $P_c^{\pm}$ state can be excluded, an additional systematic uncertainty is assigned as the difference between the least and the most significant hypotheses. Finally, the uncertainty associated with the efficiency parametrization is evaluated by summing two contributions. The first is obtained by replacing the default efficiency map with one determined from simulation of different data-taking conditions, and the second by using a parametrization given by the product of one-dimensional functions of the considered fit variables. Other systematic uncertainties include alternative parametrization of the background shape and the uncertainty in the background normalization, which is varied within its statistical uncertainty. The background is parametrized using data in a sideband region around the B_s^0 invariant-mass peak with $m(J/\psi p\bar{p}) \in [5300, 5350]$ MeV and $m(J/\psi p\bar{p}) \in [5420, 5460]$ MeV, to account for variations of the background as a function of the invariant mass. The default value of the hadron radius size for the Blatt-Weisskopf coefficients [42], equal to 3 GeV^{-1}, is replaced by two alternate values, 1.5 and 5 GeV^{-1}. Fit biases in the parameters estimation are extracted from the residual distribution of the generated and fitted parameters of pseudoexperiments based on the default model. Systematic uncertainties from orbital momentum for the NR, P_c contributions, and invariant-mass resolution are found to be negligible. More details about systematic uncertainties can be found in the Supplemental Material [33]. The final significance including systematic uncertainties is equal to 3.1σ, which is the minimal value among the different sources of systematic uncertainty, as reported in Table I.

TABLE I. Systematic uncertainties associated to the mass M_{P_c} (in MeV), width Γ_{P_c} (in MeV), modulus of coupling $A(P_c)$, fit fractions $f(P_c)$ (in %), p values, and associated significance (σ) of the $P_c^{\pm}$ state.

Source	M_{P_c}	Γ_{P_c}	$A(P_c)$	$f(P_c)$	p (%)	σ
NR(X) model	0.1	1.4	0.013	6.4	0.003	4.2
$J^P(P_c)$ assignment	2	12	0.100	5.5	0.2	3.1
Efficiency	0.2	4	0.012	0.4	0.001	4.4
Background	0.1	2	0.001	0.7	0.001	4.3
Hadron radius	0.7	4	0.034	1.7	0.02	3.7
Fit bias	$^{+0.2}_{-0.1}$	$^{+5}_{-2}$	$^{+0.040}_{-0.040}$	...	...	...
Total	2	14	0.11	8.6	...	3.1

The mass and width of this new pentaquarklike state are measured to be

$$M_{P_c} = 4337^{+7\ +2}_{-4\ -2}\ \text{MeV},$$
$$\Gamma_{P_c} = 29^{+26\ +14}_{-12\ -14}\ \text{MeV}, \quad (3)$$

where the first uncertainty is statistical and the second systematic. The analysis of flavor-untagged B_s^0 decays is not sensitive to the P_c^+ and P_c^- contributions separately; therefore, a single coupling is determined, which has modulus $A(P_c) = 0.19^{+0.19\ +0.11}_{-0.08\ -0.11}$ and phase $\phi(P_c)$ consistent with zero, corresponding to a fit fraction of $(22.0^{+8.5}_{-4.0} \pm 8.6)\%$ for the P_c states. Because of the limited sample size, it is not possible to distinguish among different J^P quantum numbers. A state compatible with this P_c state is predicted in Ref. [43] with $J^P = 1/2^+$.

In conclusion, an amplitude analysis of $B_s^0 \to J/\psi p\bar{p}$ decays is presented, using data collected with the LHCb detector between 2011 and 2018, and corresponding to an integrated luminosity of 9 fb^{-1}. No evidence is seen for either a P_c state at a mass of 4312 MeV [2] or the glueball state $f_J(2220)$ predicted in Ref. [11]. Unlike in other B decays [44–47], no threshold enhancement is observed in the $p\bar{p}$ invariant-mass spectrum, which is well modeled by a nonresonant contribution. Evidence for a Breit-Wigner shaped resonance in the $J/\psi p$ and $J/\psi\bar{p}$ invariant masses is obtained with a statistical significance in the range of 3.1 to 3.7σ, depending on the assigned J^P hypothesis.

We express our gratitude to our colleagues in the CERN accelerator departments for the excellent performance of the LHC. We thank the technical and administrative staff at the LHCb institutes. We acknowledge support from CERN and from the national agencies: CAPES, CNPq, FAPERJ, and FINEP (Brazil); MOST and NSFC (China); CNRS/IN2P3 (France); BMBF, DFG, and MPG (Germany); INFN (Italy); NWO (Netherlands); MNiSW and NCN (Poland); MEN/IFA (Romania); MSHE (Russia); MICINN (Spain); SNSF and SER (Switzerland); NASU (Ukraine); STFC (United Kingdom); DOE NP and NSF (U.S.). We acknowledge the computing resources that are provided by CERN, IN2P3 (France), KIT and DESY (Germany), INFN (Italy), SURF (Netherlands), PIC (Spain), GridPP (United Kingdom), RRCKI and Yandex LLC (Russia), CSCS (Switzerland), IFIN-HH (Romania), CBPF (Brazil), PL-GRID (Poland), and NERSC (U.S.). We are indebted to the communities behind the multiple open-source software packages on which we depend. Individual groups or members have received support from ARC and ARDC (Australia); AvH Foundation (Germany); EPLANET, Marie Skłodowska-Curie Actions, and ERC (European Union); A*MIDEX, ANR, IPhU and Labex P2IO, and Région Auvergne-Rhône-Alpes (France); Fondazione Fratelli Confalonieri (Italy); Key Research Program of Frontier Sciences of CAS, CAS PIFI, CAS CCEPP, Fundamental Research Funds for the Central Universities, and Science and Technology. Program of Guangzhou (China); RFBR, RSF, and Yandex LLC (Russia); GVA, XuntaGal, and GENCAT (Spain); the Leverhulme Trust, the Royal Society, and UKRI (United Kingdom).

[1] R. Aaij *et al.* (LHCb Collaboration), Observation of $J/\psi p$ Resonances Consistent with Pentaquark States in $\Lambda_b^0 \to J/\psi p K^-$ Decays, Phys. Rev. Lett. **115**, 072001 (2015).
[2] R. Aaij *et al.* (LHCb Collaboration), Observation of a Narrow Pentaquark State, $P_c(4312)^+$, and of Two-Peak Structure of the $P_c(4450)^+$, Phys. Rev. Lett. **122**, 222001 (2019).
[3] The charge-conjugate decay is implied, unless otherwise stated, and natural units with $\hbar = c = 1$ are used throughout the Letter.
[4] R. Aaij *et al.* (LHCb Collaboration), Evidence of a $J/\psi\Lambda$ structure and observation of excited Ξ^- states in the $\Xi_b^- \to J/\psi\Lambda K^-$ decay, Sci. Bull. **66**, 1278 (2021).
[5] A. Esposito, A. Pilloni, and A. D. Polosa, Multiquark resonances, Phys. Rep. **668**, 1 (2017).
[6] J.-M. Richard, Exotic hadrons: Review and perspectives, Few-Body Syst. **57**, 1185 (2016).
[7] F.-K. Guo, C. Hanhart, Ulf-G. Meißner, Q. Wang, Q. Zhao, and B. S. Zou, Hadronic molecules, Rev. Mod. Phys. **90**, 015004 (2018).
[8] F.-K. Guo, X.-H. Liu, and S. Sakai, Threshold cusps and triangle singularities in hadronic reactions, Prog. Part. Nucl. Phys. **112**, 103757 (2020).
[9] S. L. Olsen, T. Skwarnicki, and D. Zieminska, Nonstandard heavy mesons and baryons: Experimental evidence, Rev. Mod. Phys. **90**, 015003 (2018).
[10] R. Aaij *et al.* (LHCb Collaboration), Observation of $B^0_{(s)} \to J/\psi p\bar{p}$ Decays and Precision Measurements of the $B^0_{(s)}$ Masses, Phys. Rev. Lett. **122**, 191804 (2019).
[11] Y. K. Hsiao and C. Q. Geng, $f_J(2220)$ and hadronic $\bar{B}_s^0$ decays, Eur. Phys. J. C **75**, 101 (2015).
[12] J. L. Rosner, Low mass baryon anti-baryon enhancements in B decays, Phys. Rev. D **68**, 014004 (2003).
[13] R. Aaij *et al.* (LHCb Collaboration), LHCb detector performance, Int. J. Mod. Phys. A **30**, 1530022 (2015).
[14] R. Aaij *et al.*, Performance of the LHCb vertex locator, J. Instrum. **9**, P09007 (2014).
[15] R. Arink *et al.*, Performance of the LHCb outer tracker, J. Instrum. **9**, P01002 (2014).
[16] A. A. Alves, Jr. *et al.*, Performance of the LHCb muon system, J. Instrum. **8**, P02022 (2013).
[17] R. Aaij *et al.*, The LHCb trigger and its performance in 2011, J. Instrum. **8**, P04022 (2013).
[18] T. Sjöstrand, S. Mrenna, and P. Skands, A brief introduction to PYTHIA8.1, Comput. Phys. Commun. **178**, 852 (2008).
[19] I. Belyaev *et al.*, Handling of the generation of primary events in Gauss, the LHCb simulation framework, J. Phys. Conf. Ser. **331**, 032047 (2011).
[20] D. J. Lange, The EvtGen particle decay simulation package, Nucl. Instrum. Methods Phys. Res., Sect. A **462**, 152 (2001).
[21] N. Davidson, T. Przedzinski, and Z. Was, PHOTOS interface in C++: Technical and physics documentation, Comput. Phys. Commun. **199**, 86 (2016).

[22] J. Allison *et al.* (GEANT4 Collaboration), GEANT4 developments and applications, IEEE Trans. Nucl. Sci. **53**, 270 (2006); S. Agostinelli *et al.* (GEANT4 Collaboration), GEANT4: A simulation toolkit, Nucl. Instrum. Methods Phys. Res., Sect. A **506**, 250 (2003).
[23] M. Clemencic *et al.*, The LHCb simulation application, Gauss: Design, evolution and experience, J. Phys. Conf. Ser. **331**, 032023 (2011).
[24] R. Aaij *et al.* (LHCb Collaboration), Precision Measurement of *CP* Violation in $B_s^0 \to J/\psi K^+K^-$ Decays, Phys. Rev. Lett. **114**, 041801 (2015).
[25] W. D. Hulsbergen, Decay chain fitting with a Kalman filter, Nucl. Instrum. Methods Phys. Res., Sect. A **552**, 566 (2005).
[26] P. A. Zyla *et al.* (Particle Data Group), Review of particle physics, Prog. Theor. Exp. Phys. **2020**, 083C01 (2020), and 2021 update.
[27] L. Breiman, J. H. Friedman, R. A. Olshen, and C. J. Stone, *Classification and Regression Trees* (Wadsworth International Group, Belmont, CA, 1984).
[28] R. Aaij *et al.*, Selection and processing of calibration samples to measure the particle identification performance of the LHCb experiment in Run 2, Eur. Phys. J. Tech. Instrum. **6**, 1 (2019).
[29] T. Skwarnicki, A study of the radiative cascade transitions between the Upsilon-prime and Upsilon resonances, Ph.D. thesis, Institute of Nuclear Physics, Krakow [Report No. DESY-F31-86-02, 1986].
[30] S. U. Chung, *Spin Formalisms, 1971* (CERN, Geneva, 1969–1970).
[31] M. Jacob and G. C. Wick, On the general theory of collisions for particles with spin, Ann. Phys. (N.Y.) **7**, 404 (1959).
[32] M. Mikhasenko *et al.* (JPAC Collaboration), Dalitz-plot decomposition for three-body decays, Phys. Rev. D **101**, 034033 (2020).
[33] See Supplemental Material at http://link.aps.org/supplemental/10.1103/PhysRevLett.128.062001 for details on the amplitude model, the event-by-event parametrization of the efficiency, the significance studies of the different spin-parity assumptions of the P_c state, the systematic uncertainties, the distribution of the phase space, and the distributions of the maxima and minima of the $J/\psi p$ and $J/\psi \bar{p}$ invariant masses.
[34] J. Z. Bai *et al.* (BES Collaboration), Studies of $\xi(2230)$ in J/ψ Radiative Decays, Phys. Rev. Lett. **76**, 3502 (1996).
[35] M. Ablikim *et al.* (BES Collaboration), Observation of a Resonance $X(1835)$ in $J/\psi \to \gamma\pi^+\pi^-\eta'$, Phys. Rev. Lett. **95**, 262001 (2005).
[36] M. Ablikim *et al.* (BESIII Collaboration), Spin-Parity Analysis of $p\bar{p}$ Mass Threshold Structure in J/ψ and ψ' Radiative Decays, Phys. Rev. Lett. **108**, 112003 (2012).
[37] R. Aaij *et al.* (LHCb Collaboration), Study of *CP* violation in $B^\mp \to Dh^\mp$ ($h = K$, π) with the modes $D \to K^\mp\pi^\pm\pi^0$, $D \to \pi^+\pi^-\pi^0$ and $D \to K^+K^-\pi^0$, Phys. Rev. D **91**, 112014 (2015).
[38] D. Marangotto, Helicity amplitudes for generic multibody particle decays featuring multiple decay chains, Adv. High Energy Phys. **2020**, 6674595 (2020).
[39] M. Wang *et al.*, A novel method to test particle ordering and final state alignment in helicity formalism, Chin. Phys. C **45**, 063103 (2021).
[40] A. L. Read, Presentation of search results: The CL_s technique, J. Phys. G **28**, 2693 (2002).
[41] F. James, *Statistical Methods in Experimental Physics*, 2nd ed. (World Scientific, Singapore, 2006).
[42] N. Wu, Centrifugal-barrier effects and determination of interaction radius, Commun. Theor. Phys. **61**, 89 (2014).
[43] C.-W. Shen, D. Rönchen, U.-G. Meißner, and B.-S. Zou, Exploratory study of possible resonances in heavy meson-heavy baryon coupled-channel interactions, Chin. Phys. C **42**, 023106 (2018).
[44] K. Abe *et al.* (Belle Collaboration), Observation of $\bar{B}^0 \to D^{(*)0}p\bar{p}$, Phys. Rev. Lett. **89**, 151802 (2002).
[45] M. Z. Wang *et al.* (Belle Collaboration), Observation of $B^+ \to p\bar{p}\pi^+$, $B^0 \to p\bar{p}K^0$, and $B^+ \to p\bar{p}K^{*+}$, Phys. Rev. Lett. **92**, 131801 (2004).
[46] B. Aubert *et al.* (*BABAR* Collaboration), Measurement of the $B^+ \to p\bar{p}K^+$ branching fraction and study of the decay dynamics, Phys. Rev. D **72**, 051101 (2005).
[47] R. Aaij *et al.* (LHCb Collaboration), Measurements of the branching fractions of $B^+ \to p\bar{p}K^+$ decays, Eur. Phys. J. C **73**, 2462 (2013).

R. Aaij,[32] A. S. W. Abdelmotteleb,[56] C. Abellán Beteta,[50] T. Ackernley,[60] B. Adeva,[46] M. Adinolfi,[54] H. Afsharnia,[9] C. A. Aidala,[86] S. Aiola,[25] Z. Ajaltouni,[9] S. Akar,[65] J. Albrecht,[15] F. Alessio,[48] M. Alexander,[59] A. Alfonso Albero,[45] Z. Aliouche,[62] G. Alkhazov,[38] P. Alvarez Cartelle,[55] S. Amato,[2] J. L. Amey,[54] Y. Amhis,[11] L. An,[48] L. Anderlini,[22] A. Andreianov,[38] M. Andreotti,[21] F. Archilli,[17] A. Artamonov,[44] M. Artuso,[68] K. Arzymatov,[42] E. Aslanides,[10] M. Atzeni,[50] B. Audurier,[12] S. Bachmann,[17] M. Bachmayer,[49] J. J. Back,[56] P. Baladron Rodriguez,[46] V. Balagura,[12] W. Baldini,[21] J. Baptista Leite,[1] R. J. Barlow,[62] S. Barsuk,[11] W. Barter,[61] M. Bartolini,[24,a] F. Baryshnikov,[83] J. M. Basels,[14] S. Bashir,[34] G. Bassi,[29] B. Batsukh,[68] A. Battig,[15] A. Bay,[49] A. Beck,[56] M. Becker,[15] F. Bedeschi,[29] I. Bediaga,[1] A. Beiter,[68] V. Belavin,[42] S. Belin,[27] V. Bellee,[50] K. Belous,[44] I. Belov,[40] I. Belyaev,[41] G. Bencivenni,[23] E. Ben-Haim,[13] A. Berezhnoy,[40] R. Bernet,[50] D. Berninghoff,[17] H. C. Bernstein,[68] C. Bertella,[48] A. Bertolin,[28] C. Betancourt,[50] F. Betti,[48] Ia. Bezshyiko,[50] S. Bhasin,[54] J. Bhom,[35] L. Bian,[73] M. S. Bieker,[15] S. Bifani,[53] P. Billoir,[13] M. Birch,[61] F. C. R. Bishop,[55] A. Bitadze,[62] A. Bizzeti,[22,b] M. Bjørn,[63] M. P. Blago,[48] T. Blake,[56] F. Blanc,[49] S. Blusk,[68] D. Bobulska,[59] J. A. Boelhauve,[15] O. Boente Garcia,[46]

T. Boettcher,[65] A. Boldyrev,[82] A. Bondar,[43] N. Bondar,[38,48] S. Borghi,[62] M. Borisyak,[42] M. Borsato,[17] J. T. Borsuk,[35] S. A. Bouchiba,[49] T. J. V. Bowcock,[60] A. Boyer,[48] C. Bozzi,[21] M. J. Bradley,[61] S. Braun,[66] A. Brea Rodriguez,[46] M. Brodski,[48] J. Brodzicka,[35] A. Brossa Gonzalo,[56] D. Brundu,[27] A. Buonaura,[50] L. Buonincontri,[28] A. T. Burke,[62] C. Burr,[48] A. Bursche,[72] A. Butkevich,[39] J. S. Butter,[32] J. Buytaert,[48] W. Byczynski,[48] S. Cadeddu,[27] H. Cai,[73] R. Calabrese,[21,c] L. Calefice,[15,13] L. Calero Diaz,[23] S. Cali,[23] R. Calladine,[53] M. Calvi,[26,d] M. Calvo Gomez,[85] P. Camargo Magalhaes,[54] P. Campana,[23] A. F. Campoverde Quezada,[6] S. Capelli,[26,d] L. Capriotti,[20,e] A. Carbone,[20,e] G. Carboni,[31] R. Cardinale,[24,a] A. Cardini,[27] I. Carli,[4] P. Carniti,[26,d] L. Carus,[14] K. Carvalho Akiba,[32] A. Casais Vidal,[46] G. Casse,[60] M. Cattaneo,[48] G. Cavallero,[48] S. Celani,[49] J. Cerasoli,[10] D. Cervenkov,[63] A. J. Chadwick,[60] M. G. Chapman,[54] M. Charles,[13] Ph. Charpentier,[48] G. Chatzikonstantinidis,[53] C. A. Chavez Barajas,[60] M. Chefdeville,[8] C. Chen,[3] S. Chen,[4] A. Chernov,[35] V. Chobanova,[46] S. Cholak,[49] M. Chrzaszcz,[35] A. Chubykin,[38] V. Chulikov,[38] P. Ciambrone,[23] M. F. Cicala,[56] X. Cid Vidal,[46] G. Ciezarek,[48] P. E. L. Clarke,[58] M. Clemencic,[48] H. V. Cliff,[55] J. Closier,[48] J. L. Cobbledick,[62] V. Coco,[48] J. A. B. Coelho,[11] J. Cogan,[10] E. Cogneras,[9] L. Cojocariu,[37] P. Collins,[48] T. Colombo,[48] L. Congedo,[19,f] A. Contu,[27] N. Cooke,[53] G. Coombs,[59] I. Corredoira,[46] G. Corti,[48] C. M. Costa Sobral,[56] B. Couturier,[48] D. C. Craik,[64] J. Crkovská,[67] M. Cruz Torres,[1] R. Currie,[58] C. L. Da Silva,[67] S. Dadabaev,[83] L. Dai,[71] E. Dall'Occo,[15] J. Dalseno,[46] C. D'Ambrosio,[48] A. Danilina,[41] P. d'Argent,[48] J. E. Davies,[62] A. Davis,[62] O. De Aguiar Francisco,[62] K. De Bruyn,[79] S. De Capua,[62] M. De Cian,[49] J. M. De Miranda,[1] L. De Paula,[2] M. De Serio,[19,f] D. De Simone,[50] P. De Simone,[23] J. A. de Vries,[80] C. T. Dean,[67] D. Decamp,[8] L. Del Buono,[13] B. Delaney,[55] H.-P. Dembinski,[15] A. Dendek,[34] V. Denysenko,[50] D. Derkach,[82] O. Deschamps,[9] F. Desse,[11] F. Dettori,[27,g] B. Dey,[77] A. Di Cicco,[23] P. Di Nezza,[23] S. Didenko,[83] L. Dieste Maronas,[46] H. Dijkstra,[48] V. Dobishuk,[52] C. Dong,[3] A. M. Donohoe,[18] F. Dordei,[27] A. C. dos Reis,[1] L. Douglas,[59] A. Dovbnya,[51] A. G. Downes,[8] M. W. Dudek,[35] L. Dufour,[48] V. Duk,[78] P. Durante,[48] J. M. Durham,[67] D. Dutta,[62] A. Dziurda,[35] A. Dzyuba,[38] S. Easo,[57] U. Egede,[69] V. Egorychev,[41] S. Eidelman,[43,h] S. Eisenhardt,[58] S. Ek-In,[49] L. Eklund,[59,i] S. Ely,[68] A. Ene,[37] E. Epple,[67] S. Escher,[14] J. Eschle,[50] S. Esen,[13] T. Evans,[48] A. Falabella,[20] J. Fan,[3] Y. Fan,[6] B. Fang,[73] S. Farry,[60] D. Fazzini,[26,d] M. Féo,[48] A. Fernandez Prieto,[46] A. D. Fernez,[66] F. Ferrari,[20,e] L. Ferreira Lopes,[49] F. Ferreira Rodrigues,[2] S. Ferreres Sole,[32] M. Ferrillo,[50] M. Ferro-Luzzi,[48] S. Filippov,[39] R. A. Fini,[19] M. Fiorini,[21,c] M. Firlej,[34] K. M. Fischer,[63] D. S. Fitzgerald,[86] C. Fitzpatrick,[62] T. Fiutowski,[34] A. Fkiaras,[48] F. Fleuret,[12] M. Fontana,[13] F. Fontanelli,[24,a] R. Forty,[48] D. Foulds-Holt,[55] V. Franco Lima,[60] M. Franco Sevilla,[66] M. Frank,[48] E. Franzoso,[21] G. Frau,[17] C. Frei,[48] D. A. Friday,[59] J. Fu,[25,6] Q. Fuehring,[15] W. Funk,[48] E. Gabriel,[32] T. Gaintseva,[42] A. Gallas Torreira,[46] D. Galli,[20,e] S. Gambetta,[58,48] Y. Gan,[3] M. Gandelman,[2] P. Gandini,[25] Y. Gao,[5] M. Garau,[27] L. M. Garcia Martin,[56] P. Garcia Moreno,[45] J. García Pardiñas,[26,d] B. Garcia Plana,[46] F. A. Garcia Rosales,[12] L. Garrido,[45] C. Gaspar,[48] R. E. Geertsema,[32] D. Gerick,[17] L. L. Gerken,[15] E. Gersabeck,[62] M. Gersabeck,[62] T. Gershon,[56] D. Gerstel,[10] Ph. Ghez,[8] V. Gibson,[55] H. K. Giemza,[36] A. L. Gilman,[63] M. Giovannetti,[23,j] A. Gioventù,[46] P. Gironella Gironell,[45] L. Giubega,[37] C. Giugliano,[21,48,c] K. Gizdov,[58] E. L. Gkougkousis,[48] V. V. Gligorov,[13] C. Göbel,[70] E. Golobardes,[85] D. Golubkov,[41] A. Golutvin,[61,83] A. Gomes,[1,k] S. Gomez Fernandez,[45] F. Goncalves Abrantes,[63] M. Goncerz,[35] G. Gong,[3] P. Gorbounov,[41] I. V. Gorelov,[40] C. Gotti,[26] E. Govorkova,[48] J. P. Grabowski,[17] T. Grammatico,[13] L. A. Granado Cardoso,[48] E. Graugés,[45] E. Graverini,[49] G. Graziani,[22] A. Grecu,[37] L. M. Greeven,[32] N. A. Grieser,[4] P. Griffith,[21,c] L. Grillo,[62] S. Gromov,[83] B. R. Gruberg Cazon,[63] C. Gu,[3] M. Guarise,[21] P. A. Günther,[17] E. Gushchin,[39] A. Guth,[14] Y. Guz,[44] T. Gys,[48] T. Hadavizadeh,[69] G. Haefeli,[49] C. Haen,[48] J. Haimberger,[48] T. Halewood-leagas,[60] P. M. Hamilton,[66] J. P. Hammerich,[60] Q. Han,[7] X. Han,[17] T. H. Hancock,[63] S. Hansmann-Menzemer,[17] N. Harnew,[63] T. Harrison,[60] C. Hasse,[48] M. Hatch,[48] J. He,[6,l] M. Hecker,[61] K. Heijhoff,[32] K. Heinicke,[15] A. M. Hennequin,[48] K. Hennessy,[60] L. Henry,[48] J. Heuel,[14] A. Hicheur,[2] D. Hill,[49] M. Hilton,[62] S. E. Hollitt,[15] J. Hu,[17] J. Hu,[72] W. Hu,[7] X. Hu,[3] W. Huang,[6] X. Huang,[73] W. Hulsbergen,[32] R. J. Hunter,[56] M. Hushchyn,[82] D. Hutchcroft,[60] D. Hynds,[32] P. Ibis,[15] M. Idzik,[34] D. Ilin,[38] P. Ilten,[65] A. Inglessi,[38] A. Ishteev,[83] K. Ivshin,[38] R. Jacobsson,[48] S. Jakobsen,[48] E. Jans,[32] B. K. Jashal,[47] A. Jawahery,[66] V. Jevtic,[15] F. Jiang,[3] M. John,[63] D. Johnson,[48] C. R. Jones,[55] T. P. Jones,[56] B. Jost,[48] N. Jurik,[48] S. H. Kalavan Kadavath,[34] S. Kandybei,[51] Y. Kang,[3] M. Karacson,[48] M. Karpov,[82] F. Keizer,[48] M. Kenzie,[56] T. Ketel,[33] B. Khanji,[15] A. Kharisova,[84] S. Kholodenko,[44] T. Kirn,[14] V. S. Kirsebom,[49] O. Kitouni,[64] S. Klaver,[32] K. Klimaszewski,[36] M. R. Kmiec,[36] S. Koliiev,[52] A. Kondybayeva,[83] A. Konoplyannikov,[41] P. Kopciewicz,[34] R. Kopecna,[17] P. Koppenburg,[32] M. Korolev,[40] I. Kostiuk,[32,52] O. Kot,[52] S. Kotriakhova,[21,38] P. Kravchenko,[38] L. Kravchuk,[39] R. D. Krawczyk,[48] M. Kreps,[56] F. Kress,[61] S. Kretzschmar,[14] P. Krokovny,[43,h] W. Krupa,[34] W. Krzemien,[36] W. Kucewicz,[35,m] M. Kucharczyk,[35] V. Kudryavtsev,[43,h] H. S. Kuindersma,[32,33] G. J. Kunde,[67] T. Kvaratskheliya,[41] D. Lacarrere,[48] G. Lafferty,[62] A. Lai,[27] A. Lampis,[27] D. Lancierini,[50] J. J. Lane,[62] R. Lane,[54] G. Lanfranchi,[23] C. Langenbruch,[14] J. Langer,[15]

O. Lantwin,[83] T. Latham,[56] F. Lazzari,[29,n] R. Le Gac,[10] S. H. Lee,[86] R. Lefèvre,[9] A. Leflat,[40] S. Legotin,[83] O. Leroy,[10] T. Lesiak,[35] B. Leverington,[17] H. Li,[72] P. Li,[17] S. Li,[7] Y. Li,[4] Y. Li,[4] Z. Li,[68] X. Liang,[68] T. Lin,[61] R. Lindner,[48] V. Lisovskyi,[15] R. Litvinov,[27] G. Liu,[72] H. Liu,[6] S. Liu,[4] A. Lobo Salvia,[45] A. Loi,[27] J. Lomba Castro,[46] I. Longstaff,[59] J. H. Lopes,[2] S. Lopez Solino,[46] G. H. Lovell,[55] Y. Lu,[4] D. Lucchesi,[28,o] S. Luchuk,[39] M. Lucio Martinez,[32] V. Lukashenko,[32,52] Y. Luo,[3] A. Lupato,[62] E. Luppi,[21,c] O. Lupton,[56] A. Lusiani,[29,p] X. Lyu,[6] L. Ma,[4] R. Ma,[6] S. Maccolini,[20,e] F. Machefert,[11] F. Maciuc,[37] V. Macko,[49] P. Mackowiak,[15] S. Maddrell-Mander,[54] O. Madejczyk,[34] L. R. Madhan Mohan,[54] O. Maev,[38] A. Maevskiy,[82] D. Maisuzenko,[38] M. W. Majewski,[34] J. J. Malczewski,[35] S. Malde,[63] B. Malecki,[48] A. Malinin,[81] T. Maltsev,[43,h] H. Malygina,[17] G. Manca,[27,g] G. Mancinelli,[10] D. Manuzzi,[20,e] D. Marangotto,[25,q] J. Maratas,[9,r] J. F. Marchand,[8] U. Marconi,[20] S. Mariani,[22,s] C. Marin Benito,[48] M. Marinangeli,[49] J. Marks,[17] A. M. Marshall,[54] P. J. Marshall,[60] G. Martellotti,[30] L. Martinazzoli,[48,d] M. Martinelli,[26,d] D. Martinez Santos,[46] F. Martinez Vidal,[47] A. Massafferri,[1] M. Materok,[14] R. Matev,[48] A. Mathad,[50] Z. Mathe,[48] V. Matiunin,[41] C. Matteuzzi,[26] K. R. Mattioli,[86] A. Mauri,[32] E. Maurice,[12] J. Mauricio,[45] M. Mazurek,[48] M. McCann,[61] L. Mcconnell,[18] T. H. Mcgrath,[62] N. T. Mchugh,[59] A. McNab,[62] R. McNulty,[18] J. V. Mead,[60] B. Meadows,[65] G. Meier,[15] N. Meinert,[76] D. Melnychuk,[36] S. Meloni,[26,d] M. Merk,[32,80] A. Merli,[25,q] L. Meyer Garcia,[2] M. Mikhasenko,[48] D. A. Milanes,[74] E. Millard,[56] M. Milovanovic,[48] M.-N. Minard,[8] A. Minotti,[21] L. Minzoni,[21,c] S. E. Mitchell,[58] B. Mitreska,[62] D. S. Mitzel,[48] A. Mödden,[15] R. A. Mohammed,[63] R. D. Moise,[61] T. Mombächer,[46] I. A. Monroy,[74] S. Monteil,[9] M. Morandin,[28] G. Morello,[23] M. J. Morello,[29,p] J. Moron,[34] A. B. Morris,[75] A. G. Morris,[56] R. Mountain,[68] H. Mu,[3] F. Muheim,[58,48] M. Mulder,[48] D. Müller,[48] K. Müller,[50] C. H. Murphy,[63] D. Murray,[62] P. Muzzetto,[27,48] P. Naik,[54] T. Nakada,[49] R. Nandakumar,[57] T. Nanut,[49] I. Nasteva,[2] M. Needham,[58] I. Neri,[21] N. Neri,[25,q] S. Neubert,[75] N. Neufeld,[48] R. Newcombe,[61] T. D. Nguyen,[49] C. Nguyen-Mau,[49,t] E. M. Niel,[11] S. Nieswand,[14] N. Nikitin,[40] N. S. Nolte,[64] C. Normand,[8] C. Nunez,[86] A. Oblakowska-Mucha,[34] V. Obraztsov,[44] T. Oeser,[14] D. P. O'Hanlon,[54] S. Okamura,[21] R. Oldeman,[27,g] M. E. Olivares,[68] C. J. G. Onderwater,[79] R. H. O'neil,[58] A. Ossowska,[35] J. M. Otalora Goicochea,[2] T. Ovsiannikova,[41] P. Owen,[50] A. Oyanguren,[47] K. O. Padeken,[75] B. Pagare,[56] P. R. Pais,[48] T. Pajero,[63] A. Palano,[19] M. Palutan,[23] Y. Pan,[62] G. Panshin,[84] A. Papanestis,[57] M. Pappagallo,[19,f] L. L. Pappalardo,[21,c] C. Pappenheimer,[65] W. Parker,[66] C. Parkes,[62] B. Passalacqua,[21] G. Passaleva,[22] A. Pastore,[19] M. Patel,[61] C. Patrignani,[20,e] C. J. Pawley,[80] A. Pearce,[48] A. Pellegrino,[32] M. Pepe Altarelli,[48] S. Perazzini,[20] D. Pereima,[41] A. Pereiro Castro,[46] P. Perret,[9] M. Petric,[59,48] K. Petridis,[54] A. Petrolini,[24,a] A. Petrov,[81] S. Petrucci,[58] M. Petruzzo,[25] T. T. H. Pham,[68] A. Philippov,[42] L. Pica,[29,p] M. Piccini,[78] B. Pietrzyk,[8] G. Pietrzyk,[49] M. Pili,[63] A. Pilloni,[30,u] D. Pinci,[30] F. Pisani,[48] M. Pizzichemi,[26,48,d] V. Placinta,[37] J. Plews,[53] M. Plo Casasus,[46] F. Polci,[13] M. Poli Lener,[23] M. Poliakova,[68] A. Poluektov,[10] N. Polukhina,[83,v] I. Polyakov,[68] E. Polycarpo,[2] S. Ponce,[48] D. Popov,[6,48] S. Popov,[42] S. Poslavskii,[44] K. Prasanth,[35] L. Promberger,[48] C. Prouve,[46] V. Pugatch,[52] V. Puill,[11] H. Pullen,[63] G. Punzi,[29,w] H. Qi,[3] W. Qian,[6] J. Qin,[6] N. Qin,[3] R. Quagliani,[13] B. Quintana,[8] N. V. Raab,[18] R. I. Rabadan Trejo,[10] B. Rachwal,[34] J. H. Rademacker,[54] M. Rama,[29] M. Ramos Pernas,[56] M. S. Rangel,[2] F. Ratnikov,[42,82] G. Raven,[33] M. Reboud,[8] F. Redi,[49] F. Reiss,[62] C. Remon Alepuz,[47] Z. Ren,[3] V. Renaudin,[63] P. K. Resmi,[10] R. Ribatti,[29] S. Ricciardi,[57] K. Rinnert,[60] P. Robbe,[11] G. Robertson,[58] A. B. Rodrigues,[49] E. Rodrigues,[60] J. A. Rodriguez Lopez,[74] E. R. R. Rodriguez Rodriguez,[46] A. Rollings,[63] P. Roloff,[48] V. Romanovskiy,[44] M. Romero Lamas,[46] A. Romero Vidal,[46] J. D. Roth,[86] M. Rotondo,[23] M. S. Rudolph,[68] T. Ruf,[48] R. A. Ruiz Fernandez,[46] J. Ruiz Vidal,[47] A. Ryzhikov,[82] J. Ryzka,[34] J. J. Saborido Silva,[46] N. Sagidova,[38] N. Sahoo,[56] B. Saitta,[27,g] M. Salomoni,[48] C. Sanchez Gras,[32] R. Santacesaria,[30] C. Santamarina Rios,[46] M. Santimaria,[23] E. Santovetti,[31,j] D. Saranin,[83] G. Sarpis,[14] M. Sarpis,[75] A. Sarti,[30] C. Satriano,[30,x] A. Satta,[31] M. Saur,[15] D. Savrina,[41,40] H. Sazak,[9] L. G. Scantlebury Smead,[63] A. Scarabotto,[13] S. Schael,[14] S. Scherl,[60] M. Schiller,[59] H. Schindler,[48] M. Schmelling,[16] B. Schmidt,[48] O. Schneider,[49] A. Schopper,[48] M. Schubiger,[32] S. Schulte,[49] M. H. Schune,[11] R. Schwemmer,[48] B. Sciascia,[23] S. Sellam,[46] A. Semennikov,[41] M. Senghi Soares,[33] A. Sergi,[24,a] N. Serra,[50] L. Sestini,[28] A. Seuthe,[15] P. Seyfert,[48] Y. Shang,[5] D. M. Shangase,[86] M. Shapkin,[44] I. Shchemerov,[83] L. Shchutska,[49] T. Shears,[60] L. Shekhtman,[43,h] Z. Shen,[5] V. Shevchenko,[81] E. B. Shields,[26,d] Y. Shimizu,[11] E. Shmanin,[83] J. D. Shupperd,[68] B. G. Siddi,[21] R. Silva Coutinho,[50] G. Simi,[28] S. Simone,[19,f] N. Skidmore,[62] T. Skwarnicki,[68] M. W. Slater,[53] I. Slazyk,[21,c] J. C. Smallwood,[63] J. G. Smeaton,[55] A. Smetkina,[41] E. Smith,[50] M. Smith,[61] A. Snoch,[32] M. Soares,[20] L. Soares Lavra,[9] M. D. Sokoloff,[65] F. J. P. Soler,[59] A. Solovev,[38] I. Solovyev,[38] F. L. Souza De Almeida,[2] B. Souza De Paula,[2] B. Spaan,[15] E. Spadaro Norella,[25,q] P. Spradlin,[59] F. Stagni,[48] M. Stahl,[65] S. Stahl,[48] S. Stanislaus,[63] O. Steinkamp,[50,83] O. Stenyakin,[44] H. Stevens,[15] S. Stone,[68] M. E. Stramaglia,[49] M. Straticiuc,[37] D. Strekalina,[83] F. Suljik,[63] J. Sun,[27] L. Sun,[73] Y. Sun,[66] P. Svihra,[62] P. N. Swallow,[53] K. Swientek,[34] A. Szabelski,[36] T. Szumlak,[34] M. Szymanski,[48] S. Taneja,[62] A. R. Tanner,[54]

M. D. Tat,[63] A. Terentev,[83] F. Teubert,[48] E. Thomas,[48] D. J. D. Thompson,[53] K. A. Thomson,[60] V. Tisserand,[9] S. T'Jampens,[8] M. Tobin,[4] L. Tomassetti,[21,c] X. Tong,[5] D. Torres Machado,[1] D. Y. Tou,[13] M. T. Tran,[49] E. Trifonova,[83] C. Trippl,[49] G. Tuci,[29,w] A. Tully,[49] N. Tuning,[32,48] A. Ukleja,[36] D. J. Unverzagt,[17] E. Ursov,[83] A. Usachov,[32] A. Ustyuzhanin,[42,82] U. Uwer,[17] A. Vagner,[84] V. Vagnoni,[20] A. Valassi,[48] G. Valenti,[20] N. Valls Canudas,[85] M. van Beuzekom,[32] M. Van Dijk,[49] E. van Herwijnen,[83] C. B. Van Hulse,[18] M. van Veghel,[79] R. Vazquez Gomez,[45] P. Vazquez Regueiro,[46] C. Vázquez Sierra,[48] S. Vecchi,[21] J. J. Velthuis,[54] M. Veltri,[22,y] A. Venkateswaran,[68] M. Veronesi,[32] M. Vesterinen,[56] D. Vieira,[65] M. Vieites Diaz,[49] H. Viemann,[76] X. Vilasis-Cardona,[85] E. Vilella Figueras,[60] A. Villa,[20] P. Vincent,[13] F. C. Volle,[11] D. Vom Bruch,[10] A. Vorobyev,[38] V. Vorobyev,[43,h] N. Voropaev,[38] K. Vos,[80] R. Waldi,[17] J. Walsh,[29] C. Wang,[17] J. Wang,[5] J. Wang,[4] J. Wang,[3] J. Wang,[73] M. Wang,[3] R. Wang,[54] Y. Wang,[7] Z. Wang,[50] Z. Wang,[3] J. A. Ward,[56] H. M. Wark,[60] N. K. Watson,[53] S. G. Weber,[13] D. Websdale,[61] C. Weisser,[64] B. D. C. Westhenry,[54] D. J. White,[62] M. Whitehead,[54] A. R. Wiederhold,[56] D. Wiedner,[15] G. Wilkinson,[63] M. Wilkinson,[68] I. Williams,[55] M. Williams,[64] M. R. J. Williams,[58] F. F. Wilson,[57] W. Wislicki,[36] M. Witek,[35] L. Witola,[17] G. Wormser,[11] S. A. Wotton,[55] H. Wu,[68] K. Wyllie,[48] Z. Xiang,[6] D. Xiao,[7] Y. Xie,[7] A. Xu,[5] J. Xu,[6] L. Xu,[3] M. Xu,[7] Q. Xu,[6] Z. Xu,[5] Z. Xu,[6] D. Yang,[3] S. Yang,[6] Y. Yang,[6] Z. Yang,[5] Z. Yang,[66] Y. Yao,[68] L. E. Yeomans,[60] H. Yin,[7] J. Yu,[71] X. Yuan,[68] O. Yushchenko,[44] E. Zaffaroni,[49] M. Zavertyaev,[16,v] M. Zdybal,[35] O. Zenaiev,[48] M. Zeng,[3] D. Zhang,[7] L. Zhang,[3] S. Zhang,[71] S. Zhang,[5] Y. Zhang,[5] Y. Zhang,[63] A. Zharkova,[83] A. Zhelezov,[17] Y. Zheng,[6] T. Zhou,[5] X. Zhou,[6] Y. Zhou,[6] V. Zhovkovska,[11] X. Zhu,[3] Z. Zhu,[6] V. Zhukov,[14,40] J. B. Zonneveld,[58] Q. Zou,[4] S. Zucchelli,[20,e] D. Zuliani,[28] and G. Zunica[62]

(LHCb Collaboration)

[1]*Centro Brasileiro de Pesquisas Físicas (CBPF), Rio de Janeiro, Brazil*
[2]*Universidade Federal do Rio de Janeiro (UFRJ), Rio de Janeiro, Brazil*
[3]*Center for High Energy Physics, Tsinghua University, Beijing, China*
[4]*Institute Of High Energy Physics (IHEP), Beijing, China*
[5]*School of Physics State Key Laboratory of Nuclear Physics and Technology, Peking University, Beijing, China*
[6]*University of Chinese Academy of Sciences, Beijing, China*
[7]*Institute of Particle Physics, Central China Normal University, Wuhan, Hubei, China*
[8]*Univ. Savoie Mont Blanc, CNRS, IN2P3-LAPP, Annecy, France*
[9]*Université Clermont Auvergne, CNRS/IN2P3, LPC, Clermont-Ferrand, France*
[10]*Aix Marseille Univ, CNRS/IN2P3, CPPM, Marseille, France*
[11]*Université Paris-Saclay, CNRS/IN2P3, IJCLab, Orsay, France*
[12]*Laboratoire Leprince-Ringuet, CNRS/IN2P3, Ecole Polytechnique, Institut Polytechnique de Paris, Palaiseau, France*
[13]*LPNHE, Sorbonne Université, Paris Diderot Sorbonne Paris Cité, CNRS/IN2P3, Paris, France*
[14]*I. Physikalisches Institut, RWTH Aachen University, Aachen, Germany*
[15]*Fakultät Physik, Technische Universität Dortmund, Dortmund, Germany*
[16]*Max-Planck-Institut für Kernphysik (MPIK), Heidelberg, Germany*
[17]*Physikalisches Institut, Ruprecht-Karls-Universität Heidelberg, Heidelberg, Germany*
[18]*School of Physics, University College Dublin, Dublin, Ireland*
[19]*INFN Sezione di Bari, Bari, Italy*
[20]*INFN Sezione di Bologna, Bologna, Italy*
[21]*INFN Sezione di Ferrara, Ferrara, Italy*
[22]*INFN Sezione di Firenze, Firenze, Italy*
[23]*INFN Laboratori Nazionali di Frascati, Frascati, Italy*
[24]*INFN Sezione di Genova, Genova, Italy*
[25]*INFN Sezione di Milano, Milano, Italy*
[26]*INFN Sezione di Milano-Bicocca, Milano, Italy*
[27]*INFN Sezione di Cagliari, Monserrato, Italy*
[28]*Universita degli Studi di Padova, Universita e INFN, Padova, Padova, Italy*
[29]*INFN Sezione di Pisa, Pisa, Italy*
[30]*INFN Sezione di Roma La Sapienza, Roma, Italy*
[31]*INFN Sezione di Roma Tor Vergata, Roma, Italy*
[32]*Nikhef National Institute for Subatomic Physics, Amsterdam, Netherlands*
[33]*Nikhef National Institute for Subatomic Physics and VU University Amsterdam, Amsterdam, Netherlands*
[34]*AGH—University of Science and Technology, Faculty of Physics and Applied Computer Science, Kraków, Poland*
[35]*Henryk Niewodniczanski Institute of Nuclear Physics Polish Academy of Sciences, Kraków, Poland*

[36]National Center for Nuclear Research (NCBJ), Warsaw, Poland
[37]Horia Hulubei National Institute of Physics and Nuclear Engineering, Bucharest-Magurele, Romania
[38]Petersburg Nuclear Physics Institute NRC Kurchatov Institute (PNPI NRC KI), Gatchina, Russia
[39]Institute for Nuclear Research of the Russian Academy of Sciences (INR RAS), Moscow, Russia
[40]Institute of Nuclear Physics, Moscow State University (SINP MSU), Moscow, Russia
[41]Institute of Theoretical and Experimental Physics NRC Kurchatov Institute (ITEP NRC KI), Moscow, Russia
[42]Yandex School of Data Analysis, Moscow, Russia
[43]Budker Institute of Nuclear Physics (SB RAS), Novosibirsk, Russia
[44]Institute for High Energy Physics NRC Kurchatov Institute (IHEP NRC KI), Protvino, Russia
[45]ICCUB, Universitat de Barcelona, Barcelona, Spain
[46]Instituto Galego de Física de Altas Enerxías (IGFAE), Universidade de Santiago de Compostela, Santiago de Compostela, Spain
[47]Instituto de Fisica Corpuscular, Centro Mixto Universidad de Valencia—CSIC, Valencia, Spain
[48]European Organization for Nuclear Research (CERN), Geneva, Switzerland
[49]Institute of Physics, Ecole Polytechnique Fédérale de Lausanne (EPFL), Lausanne, Switzerland
[50]Physik-Institut, Universität Zürich, Zürich, Switzerland
[51]NSC Kharkiv Institute of Physics and Technology (NSC KIPT), Kharkiv, Ukraine
[52]Institute for Nuclear Research of the National Academy of Sciences (KINR), Kyiv, Ukraine
[53]University of Birmingham, Birmingham, United Kingdom
[54]H.H. Wills Physics Laboratory, University of Bristol, Bristol, United Kingdom
[55]Cavendish Laboratory, University of Cambridge, Cambridge, United Kingdom
[56]Department of Physics, University of Warwick, Coventry, United Kingdom
[57]STFC Rutherford Appleton Laboratory, Didcot, United Kingdom
[58]School of Physics and Astronomy, University of Edinburgh, Edinburgh, United Kingdom
[59]School of Physics and Astronomy, University of Glasgow, Glasgow, United Kingdom
[60]Oliver Lodge Laboratory, University of Liverpool, Liverpool, United Kingdom
[61]Imperial College London, London, United Kingdom
[62]Department of Physics and Astronomy, University of Manchester, Manchester, United Kingdom
[63]Department of Physics, University of Oxford, Oxford, United Kingdom
[64]Massachusetts Institute of Technology, Cambridge, Massachusetts, USA
[65]University of Cincinnati, Cincinnati, Ohio, USA
[66]University of Maryland, College Park, Maryland, USA
[67]Los Alamos National Laboratory (LANL), Los Alamos, USA
[68]Syracuse University, Syracuse, New York, USA
[69]School of Physics and Astronomy, Monash University, Melbourne, Australia
(associated with Department of Physics, University of Warwick, Coventry, United Kingdom)
[70]Pontifícia Universidade Católica do Rio de Janeiro (PUC-Rio), Rio de Janeiro, Brazil
[associated with Universidade Federal do Rio de Janeiro (UFRJ), Rio de Janeiro, Brazil)]
[71]Physics and Micro Electronic College, Hunan University, Changsha City, China
(associated with Institute of Particle Physics, Central China Normal University, Wuhan, Hubei, China)
[72]Guangdong Provincial Key Laboratory of Nuclear Science, Guangdong-Hong Kong Joint Laboratory of Quantum Matter, Institute of Quantum Matter, South China Normal University, Guangzhou, China
(associated with Center for High Energy Physics, Tsinghua University, Beijing, China)
[73]School of Physics and Technology, Wuhan University, Wuhan, China
(associated with Center for High Energy Physics, Tsinghua University, Beijing, China)
[74]Departamento de Fisica, Universidad Nacional de Colombia, Bogota, Colombia
(associated with LPNHE, Sorbonne Université, Paris Diderot Sorbonne Paris Cité, CNRS/IN2P3, Paris, France)
[75]Universität Bonn—Helmholtz-Institut für Strahlen und Kernphysik, Bonn, Germany
(associated with Physikalisches Institut, Ruprecht-Karls-Universität Heidelberg, Heidelberg, Germany)
[76]Institut für Physik, Universität Rostock, Rostock, Germany
(associated with Physikalisches Institut, Ruprecht-Karls-Universität Heidelberg, Heidelberg, Germany)
[77]Eotvos Lorand University, Budapest, Hungary
[associated with European Organization for Nuclear Research (CERN), Geneva, Switzerland]
[78]INFN Sezione di Perugia, Perugia, Italy
(associated with INFN Sezione di Ferrara, Ferrara, Italy)
[79]Van Swinderen Institute, University of Groningen, Groningen, Netherlands
(associated with Nikhef National Institute for Subatomic Physics, Amsterdam, Netherlands)
[80]Universiteit Maastricht, Maastricht, Netherlands
(associated with Nikhef National Institute for Subatomic Physics, Amsterdam, Netherlands)
[81]National Research Centre Kurchatov Institute, Moscow, Russia
[associated with Institute of Theoretical and Experimental Physics NRC Kurchatov Institute (ITEP NRC KI), Moscow, Russia]

[82]National Research University Higher School of Economics, Moscow, Russia
(associated with Yandex School of Data Analysis, Moscow, Russia)
[83]National University of Science and Technology "MISIS", Moscow, Russia
[associated with Institute of Theoretical and Experimental Physics NRC Kurchatov Institute (ITEP NRC KI), Moscow, Russia]
[84]National Research Tomsk Polytechnic University, Tomsk, Russia
[associated with Institute of Theoretical and Experimental Physics NRC Kurchatov Institute (ITEP NRC KI), Moscow, Russia]
[85]DS4DS, La Salle, Universitat Ramon Llull, Barcelona, Spain
(associated with ICCUB, Universitat de Barcelona, Barcelona, Spain)
[86]University of Michigan, Ann Arbor, USA
(associated with Syracuse University, Syracuse, New York, USA)

[a]Also at Università di Genova, Genova, Italy.
[b]Also at Università di Modena e Reggio Emilia, Modena, Italy.
[c]Also at Università di Ferrara, Ferrara, Italy.
[d]Also at Università di Milano Bicocca, Milano, Italy.
[e]Also at Università di Bologna, Bologna, Italy.
[f]Also at Università di Bari, Bari, Italy.
[g]Also at Università di Cagliari, Cagliari, Italy.
[h]Also at Novosibirsk State University, Novosibirsk, Russia.
[i]Also at Department of Physics and Astronomy, Uppsala University, Uppsala, Sweden.
[j]Also at Università di Roma Tor Vergata, Roma, Italy.
[k]Also at Universidade Federal do Triângulo Mineiro (UFTM), Uberaba-MG, Brazil.
[l]Also at Hangzhou Institute for Advanced Study, UCAS, Hangzhou, China.
[m]Also at AGH—University of Science and Technology, Faculty of Computer Science, Electronics and Telecommunications, Kraków, Poland.
[n]Also at Università di Siena, Siena, Italy.
[o]Also at Università di Padova, Padova, Italy.
[p]Also at Scuola Normale Superiore, Pisa, Italy.
[q]Also at Università degli Studi di Milano, Milano, Italy.
[r]Also at MSU—Iligan Institute of Technology (MSU-IIT), Iligan, Philippines.
[s]Also at Università di Firenze, Firenze, Italy.
[t]Also at Hanoi University of Science, Hanoi, Vietnam.
[u]Also at Dipartimento di Scienze Matematiche e Informatiche, Scienze Fisiche e Scienze della Terre, Università degli Studi di Messina, Messina, Italy.
[v]Also at P.N. Lebedev Physical Institute, Russian Academy of Science (LPI RAS), Moscow, Russia.
[w]Also at Università di Pisa, Pisa, Italy.
[x]Also at Università della Basilicata, Potenza, Italy.
[y]Also at Università di Urbino, Urbino, Italy.